JOURNAL OF CATALYSIS 136, 16–23 (1992)

Oxygen X-Ray Absorption Near-Edge Structure Characterization of the Ba-Doped Yttria Oxidative Coupling Catalyst

M. P. KAMINSKY,* G. W. ZAJAC,* J. C. CAMPUZANO,†,‡ M. FAIZ,†,‡
L. BEAULAIGUE,‡ K. GOFRON,†,‡ G. JENNINGS,‡ J. M. YAO,§ AND D. K. SALDIN§

*Amoco Chemical Corporation, P.O. Box 3011, Naperville, Illinois 60566; †Department of Physics, University of Ilinois at Chicago, P.O. Box 4348, Chicago, Illinois 60680; ‡Materials Science Division, Argonne National Laboratory, Argonne, Illinois 60439; and §Department of Physics, University of Wisconsin–Milwaukee, P.O. Box 413, Milwaukee, Wisconsin 53211

Received August 12, 1991; revised February 12, 1992

Ba-doped Y_2O_3 is one of the most active catalysts for the oxidative coupling of methane. Here, based on measurements of the oxygen *K*-edge X-ray absorption edge, X-ray diffraction, X-ray fluorescence, and X-ray photoelectron spectroscopy and its catalytic activity and selectivity, we propose that the active sites are charge-deficient oxygen sites created as Ba^{2+} substitutes into Y^{3+} lattice sites. The substitution is temperature dependent, becoming significant only at higher temperatures. We have found a correlation of catalytic activity and selectivity as a function of Ba loading on Y_2O_3. This is reflected in the oxygen *K*-edge absorption near the absorption edge.

INTRODUCTION

There is great incentive to further understand the chemistry of selectively converting methane to value-added products. New stringent clean fuel laws and uncertain crude oil supplies could motivate the use of natural gas-based fuels to supplement those based on crude oil. The most direct method of utilizing natural gas in place of simple combustion is the oxidative coupling of methane to higher hydrocarbons such as ethylene:

$$4CH_4 + O_2 \xrightarrow[\text{850°C, 1 atm}\ \text{GHSV} = 48\text{–}15\text{K/h}]{\text{Catalyst}} 2C_2H_6 + 2H_2O + \underset{(CO_2,\ CO,\ C_2H_4,\ C_3\text{–}C_7)}{\text{Other products}}$$

(Oxygen-limited)

Among the hundreds of catalysts that can be used in this reaction, Ba-doped Y_2O_3 is one of the more active, while maintaining high C_{2+} selectivity. It is thought that the addition of Ba to Y_2O_3 increases the performance of the catalyst, possibly due to the creation of charge-deficient oxygen sites as Ba^{2+} substitutes into Y^{3+} lattice sites. The resulting charge imbalance is compensated by the creation of O^- sites. Driscoll and Lunsford (*1*) and Wang and Lunsford (*2*) have speculated that these oxyen defect sites catalyze the oxidative coupling as follows: As a CH_4 molecule strikes the defect site, one H is removed, releasing a methyl radical into the gas phase, two of which couple to form ethane. The defect site converted to a hydroxide ion is then regenerated by the elimination of water followed by reoxidation from gas-phase oxygen.

Here we attempt to prove the feasibility of this model by establishing a correlation between the catalytic activity and oxygen charge deficiency as measured by the X-ray absorption near-edge structure (XANES) of the oxygen *K*-edge. XANES is a powerful tool for probing the unoccupied local density of electronic states of selected angular momentum character at the site of the absorbing atom. In these experiments we determine the catalytic activity and C_{2+} selectivity as the Ba loading level of Y_2O_3 is

0021-9517/92 $5.00

increased from 1 to 7.5 wt% while observing the XANES structure of the catalyst. The experimental XANES structure is interpreted with the help of multiple scattering model calculations of the near-edge absorption spectrum of the oxygen sublattice of Ba/Y_2O_3 as a function of Ba substitution into the Y sites. Recently, XANES experiments have been successfully used for characterizing the empty electronic energy levels on the oxygen sites of the new high-temperature superconductors (*3*) of the $YBa_2Cu_3O_{7-x}$ family. We have pursued the same approach in characterizing the electronic states of this mixed oxide catalytic system.

METHODS

A. Catalyst Preparation

Both the 1 and the 7.5 wt% Ba/Y_2O_3 samples were prepared by the incipient wetness technique. Pure yttria (Alfa, 99.99%) was dried in a vacuum overnight at 140°C to remove water and other volatiles. The appropriate amount of barium nitrate (Alfa, 99.9%) was dissolved into warm, distilled water, care taken to avoid exposure to CO_2 in the air. Any CO_2 exposure would cause $BaCO_3$ to precipitate out of the solution. All of the barium nitrate dissolved with gentle heating and stirring. The warm barium solution was then added dropwise to the yttria until the wetness point had been reached. The Ba/Y_2O_3 slurry was then treated to dryness before subsequent impregnations were performed to support the rest of the barium solution. After adding all of the barium nitrate solution, the Ba/Y_2O_3 catalyst was calcined in air using a $(Y)ZrO_2$ crucible. The temperature program was as follows: ramp from room temperature at 4°C/min to 400°C, hold 1 h, ramp 2°C/min to 900°C, hold 6 h, then cool.

B. Catalyst Characterization by X-Ray Diffraction and X-Ray Fluorescence

The X-ray diffraction results indicate that Y_2O_3 is the major phase present, while a small percentage of $BaCO_3$ is detected in the 7.5 wt% Ba/Y_2O_3 sample. X-ray fluorescence quantified the nominally 1 wt% Ba at 1 wt% Ba, while the nominal 10 wt% sample was measured at 7.5 wt% Ba. The atomic ratios measured by X-ray photoelectron spectroscopy, accounting for the relative sensitivities of Ba and Y, are shown in Table 1. By a simple conversion from the weight to the atomic percentage, one calculates that the ratio of Ba/Y for the 1 wt% Ba sample is 0.02 and that for the 7.5 wt% sample it is 0.15. The X-ray photoelectron spectroscopy ratios are 2–4 times higher at the surface than in the bulk, indicating surface enrichment of the barium phase on the surface of the yttria particles. This observation is consistent with the incipient wetness method of catalyst preparation mentioned in Section A. The 1 wt% Ba represents roughly 0.5–0.7 ml equivalent monolayer surface coverage. Therefore the 7.5 wt% sample should have a substantial baria contribution to the XANES signal as observed in the XPS measurement (0.24 Ba/Y).

TABLE 1

XPS Atomic Ratios

Catalyst	Ba/Y
Y_2O_3	0.0
1 wt% Ba/Y_2O_3	0.09
10 w% Ba/Y_2O_3	0.24

C. X-Ray Photoelectron Spectroscopy in Situ Treatments

We know by X-ray diffraction that a minor phase of barium carbonate is present if the catalyst is exposed to air. This is evident in the carbon 1*s* spectrum as shown in Fig. 1a. The peak at 288 eV indicates that over 50% of the carbon present at the surface is in the carbonate phase. This percentage of carbonate accounts stoichiometrically for all the barium present. If we treat the 7.5 wt% sample at 900°C in O_2 for 2 h to decompose the carbonate phase present, we observe that the carbonate is completely decomposed and roughly half of the adventi-

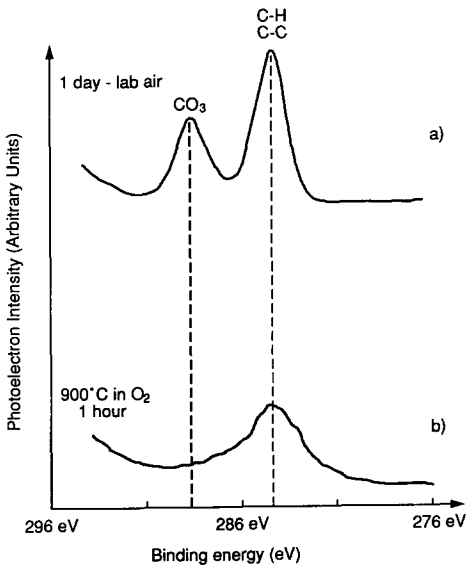

FIG. 1. (a) XPS evidence for the presence of carbonate on the Ba-doped catalyst. The carbonate is removed by heating in vacuum to 900°C, as shown in spectrum (b).

tious carbon has been oxidized from the surface, as shown in Fig. 1b.

D. Catalyst Screening

All oxidative coupling reactions were run in the co-feed mode using plug flow quartz microreactors at 850°C reaction temperature and 1 atm of pressure. The reactors were coupled to a computer-controlled on-line gas chromatograph for product analysis. Figure 2 is a schematic diagram of the reactor design. The catalysts were usually diluted 20 : 1 with α-alumina for better heat control. The reactor consisted of a 14-mm i.d. quartz tube with a 4-ml catalyst bed held in the center of the tube by a quartz wool plug and a quartz deadman. The deadman decreased the postcatalyst bed void volume, which helps limit secondary combustion reactions. A three-zone electric furnace was used to heat the catalyst bed, which was controlled by three thermocouples housed in a quartz thermowell running up the middle of the catalyst bed. Mass flow controllers were used for the gas feed and the product gases were sampled by an on-line gas chromatograph. Virtually every step of this process was computer controlled, from the temperature and flow to the gas chromatograph sampling, integration, and data management.

XANES Measurements

The powder samples were pressed into wafers 11 mm in diameter and 1 mm thick for the XANES measurements. The experiments were carried out at the Aladdin synchrotron using the Argonne–Minnesota extended range grasshopper monochromator with an energy resolution of 300 meV. Photons in the energy range 500 to 600 eV (oxygen K-edge: 530 eV) were incident on the sample at 45° from the surface normal. The total electron yield from the surface was measured by a channeltron electron multiplier situated approximately 10 cm from the surface at the complementary 45° from the surface normal. Thus secondary electron flux was approximately perpendicular to the photon flux. The photon flux was considerably smaller than the sample so that no stray electrons were present. Light coating of one of the mirrors in the beamline with a very thin layer of Cr provides a calibration absorption dip so that the edge energies are accurately known. This dip also allows accurate calibration of the absorption scale of the different spectra. The samples were

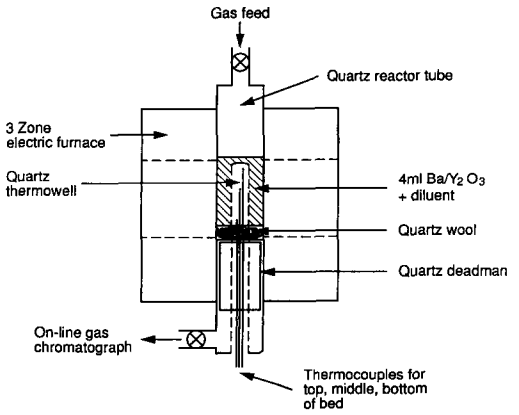

FIG. 2. Schematic diagram of the quartz microreactor.

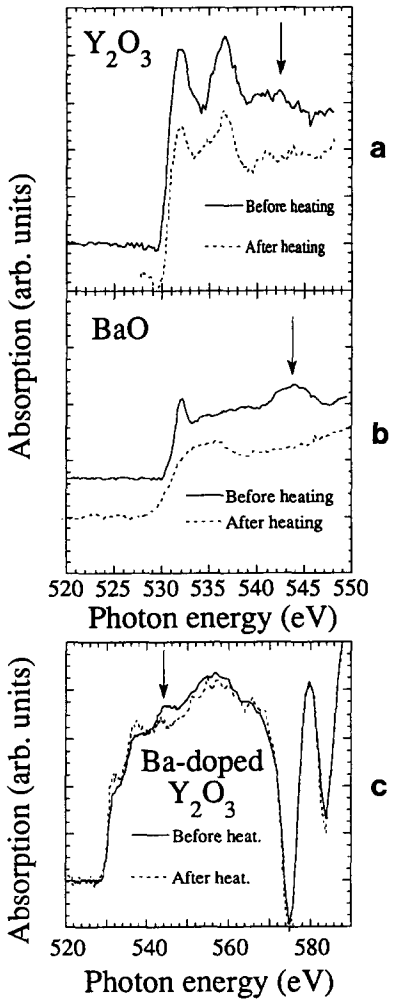

FIG. 3. XANES spectra of (a) pure Y_2O_3, (b) BaO, and (c) 7.5 wt% Ba/Y_2O_3 before and after *in situ* UHV calcination. The samples were left in air for a month after preparation and before measurement and show considerable carbonate formation, as indicated by the arrow. There is also suppression of the white line at the X-ray absorption edge. After heating the samples *in situ*, the carbonate is removed.

heated *in situ* to 900°C to remove any carbonate (which is easily detected by XANES as a peak about 12 eV above the edge, as indicated by the arrow in Fig. 3) created during sample transfer from the catalytic reactor to the XANES spectrometer. All of the spectra shown here have not been smoothed or filtered in any way and have only been normalized using the Cr (L_{II}, L_{III}) absorption dips at 583.8 and at 574.1 eV, as seen in Fig. 3. In Fig. 3, the spectra have been displaced in order to make the differences more apparent.

RESULTS

Catalytic Trends

It is important to compare catalyst C_{2+} selectivities by running the samples at near 100% oxygen conversion. This is due to the unreacted oxygen in the product stream causing secondary combustion and dehydrogenation reactions of the C_{2+} products. A high reaction temperature of 850°C was found to be optimal for this feed mixture in order to obtain the highest C_{2+} yields. As seen in Table 2, all catalysts have oxygen conversions in the 96.6% or higher range. However, this does not mean that all the catalysts have the same activity level. The difference in activities of the catalysts is indicated instead by the large variation in flow rates necessary to achieve around 100% oxygen conversion.

Oxygen K-Edge XANES

Spectra of the Y_2O_3, 1 and the 7.5 wt% Ba/Y_2O_3 samples are shown in Fig. 4. Note that the yttria spectrum has a characteristic structure near the edge region. This has been modeled by a five-shell multiple scattering calculation as discussed below. Note that as the Ba concentration increases, the peaks near the edge increase in intensity. There is also a dip in the absorption cross section before the edge, at 528.6 eV, which is due to a Fano resonance observed in metal oxides (*4*). It results from an interference of two ionization channels (*5*). As expected, the resonance increases with increased doping, as the hole density increases, enhancing the autoionization channel. It is informative to compare the oxygen *K*-edge of the 7.5 wt% Ba/Y_2O_3 sample as function of thermal treatment. In Fig. 5 we show the sample after flashing to 900°C and a spectrum taken with the sample at 600°C. Note the dramatic increase of the near-edge region absorption

TABLE 2

Catalytic Activity of Yttria and Ba-Doped Yttria

Catalyst	Gas hourly space vel.	% C_{2+} selectivity	% O_2 conversion	CH_4/O_2 ratio
10% Ba/Y_2O_3 20:1 diluent	180,000	63.2%	96.6%	5
1% Ba/Y_2O_3 20:1 diluent	164,000	61.9%	98.7%	5
Y_2O_3	~36,000	57.7%	97%	5
$BaCO_3$	12,500	62%	98%	5

at 600°C. Note from Fig. 3b that the spectrum of Ba-doped Y_2O_3 cannot be expressed as a linear combination of BaO and Y_2O_3. Thus the oxygen *K*-edge of Ba/Y_2O_3 is unique to the sample. This is an indication of a strong interaction between the surface Ba and the yttria particle. In Fig. 3b the difference in the spectra before vs after heating is due to the decomposition of the $BaCO_3$ surface phase which is observed by XPS. A pure $BaCO_3$ reference sample has been run by O *K*-edge XANES and is very similar to the unheated BaO spectrum.

DISCUSSION

Oxygen K-Edge Absorption Modeling

The XANES data provide the density of unoccupied states of particular angular momentum character as follows: an electron from a filled oxygen 1*s* state absorbs a photon and is promoted to an empty state above the highest occupied orbital. The transition will only occur if the X ray has enough energy to promote the electron to an empty level. The 1*s* hole left behind is filled by electrons from higher occupied levels, and the ensuing Auger electrons are ejected from the sample, causing a shower of inelastic secondary electrons, which we monitor as a measure of the filling of the O^- states. The selection rule for dipole transitions $\Delta L = \pm 1$ requires that when the 1*s* electron absorbs the photon, it can only make transitions to *p* orbitals centered on the oxygen atom. The lowest unoccupied of these levels

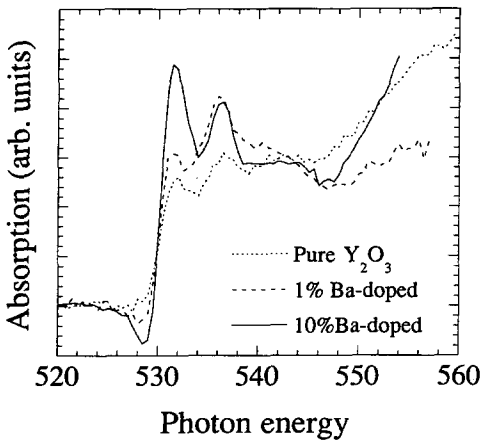

FIG. 4. XANES spectra of Y_2O_3 (---), 1% Ba/Y_2O_3 (–––), and 7.5% Ba/Y_2O_3 (—).

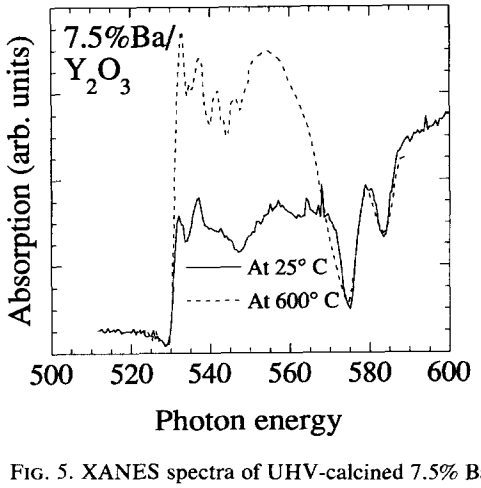

FIG. 5. XANES spectra of UHV-calcined 7.5% Ba/Y_2O_3 (—) and the spectra of the same sample at 600°C (---).

happen to be the bonding orbitals of oxygen. The interpretation of experimental data requires a computational modeling of the X-ray absorption process. We perform this modeling using the real-space multiple scattering scheme of Vvedensky *et al.* (*6*). Muffin-tin potentials of Y, Ba, and oxygen ions are generated by the Mattheiss prescription (*7*), starting from self-consistent free-atom potentials (*8*). The degree of ionicity, 0.75, assumed for each of the atoms is based on the approximate electronegativity differences between the cations and anions (*9*). The oxygen *K*-edge XANES is determined by the multiple scattering of the electrons ejected from the *K*-shells of the oxygen ions. This, in turn, depends on the nature and distribution of the ions immediately surrounding the oxygen site. Y_2O_3 has the complicated cubic bixbyite structure containing 80 atoms per unit cell. The XANES is simulated by modeling the multiple scattering of the core electrons ejected from each of the oxygen ions. This enables us to calculate the atomic transition rate as a function of the energy of the ejected electrons. The calculation was performed by dividing the surrounding cluster of atoms into a set of five concentric shells containing atoms of nearly the same distance from the absorbing atom, thus allowing the advantageous subdivision of multiple scattering paths into intrashell and intershell processes (*10*). The polycrystalline nature of the experimental samples was simulated by averaging over all directions of the X-ray polarization with respect to the crystallographic axes. The results, shown in Fig. 6a, bear good resemblance to the experimental data from pure Y_2O_3. The scattering properties of the cation sites were calculated on the basis of the average *t*-matrix approximation, where the *t*-matrices of the cation sites were taken to be $t_{av} = 0.1t_{Ba} + 0.9t_Y$, where t_{Ba} and t_Y are the *t* matrices of the Ba and Y ions, respectively. The decrease in the positive charge on the cations must be compensated by a reduction in the average negative charge of the anion sites. We consider two models that accomplish this. On the first model the negative charge on the oxygen ions is assumed to be reduced uniformly. Charge neutrality is achieved if the oxygen ionicity is reduced to -1.45. This increases the weight of the unoccupied $2p$ states on all the oxygen ions. On the second model, charge neutrality is achieved by assuming sufficient oxygen vacancies to account for the charge imbalance of 10% Ba^{2+} substitution into Y^{3+} sites. In Fig. 6b the resulting simulated XANES spectra are compared to the experimental spectrum of the 7.5 wt% Ba-doped sample. Note that the intensity of the peak closest to the absorption edge is increased relative to the second peak on both calculations and experiment, consistent with the notion of the emptying of the oxygen $2p$ states on Ba-doping. Although both models are in reasonable agreement with the experimental data,

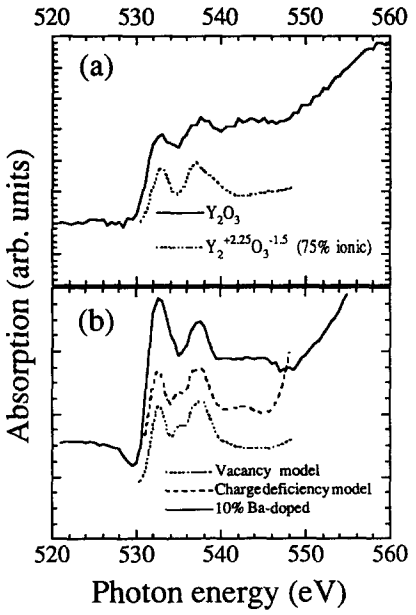

FIG. 6. Comparison of calculated and experimental XANES spectra. (a) Comparison of pure Y_2O_3 (—) and the $Y_2^{2.25+}O^{1.5-}$ model; (b) comparison of 7.5% Ba/Y_2O_3 (—) with the model of 7.5% $Ba^{1.5+}$ substitution in the Y sites of $Y_2^{2.25+}O_3^{1.45-}$ (– – –) and the model in which 7.5% $Ba^{1.5+}$ is substituted in the Y sites of $Y_2^{2.25+}O_3^{1.5-}$ with sufficient O vacancies to compensate for the charge deficiency (· · ·).

the spectrum from the charge-deficiency model is clearly closer to the data. In their computer simulations, by the same method, of the O *K*-edge in rutile, Brydson *et al.* (*11*) have found the calculated energy scale near the absorption edge to be considerably expanded compared with that of the experimental spectrum. They have ascribed the discrepancy to the energy-dependent exchange-correlation potential experienced by the excited electron in the sea of crystal electrons, which is not taken into account in the simulations. Recent calculations of this potential by Mustre de Leon *et al.* (*12*) have suggested that its effect could be to compress the theoretical energy scale close to the absorption edge, where the potential can have a negative gradient, but to expand it further away from the edge, where the gradient is always positive. The results of our simulations were consistent with the experience of Brydson *et al.* (*11*), and we have accordingly compressed the energy scale near the absorption edge to align the two prominent peaks. The misalignment of the rise in the absorption coefficient near 550 eV on the experimental spectrum compared with that of the charge-deficiency model on Fig. 6b is therefore probably due to the need to expand the theoretical curve in that region, consistent with the results of Mustre de Leon *et al.* (*12*). Although the bulk solubility of Ba in Y_2O_3 is low, the model and the data argue for a substitution, particularly at high temperatures. Although this does not uniquely define the nature of the surface site, it does indicate a charge deficiency on the oxygen sites at the surface which is substantial. Such changes in the oxygen near-edge region as a function of the charge on the oxygen site have been previously modeled for transitions metals (*13*). Those results are in accord with our findings.

Correlation of XANES Data to Catalytic Activity

There is a clear trend showing increased activity with increased Ba concentration in Y_2O_3. Pure $BaCO_3$ was much less active, although more selective, than Y_2O_3. C_{2+} selectivity also increases with increased Ba loading, although this increase was not as large as the activity increase. As discussed, there is a trend of increased C_{2+} yield with increased reaction temperature for the Ba/Y_2O_3 catalysts. This is consistent with the XANES data taken at 600°C (Fig. 5), which showed dramatic increases in step height of the edge compared to the same catalyst at room temperature. This temperature is considerably below that necessary to thermally reduce yttria (>1500°C (*14*)). Therefore, thermally generated oxygen vacancies cannot be the cause of the observed changes. In addition to the step height increase several new features appear at 600°C, possibly indicating a reversible phase change. This thermal enhancement could also be the reason that the catalyst shows significant activity only at elevated temperatures. In other words, the increase in activity at elevated temperatures is not due simply to overcoming an activation barrier, but also to an inherent change in the catalyst at elevated temperatures. We are currently investigating by means of high-temperature XRD if the changes are due to phase change in the catalyst, such as increased substitution of Ba for Y at elevated temperatures. The sample had been previously heated to decompose any carbonate phases present. The increase in near-edge absorption for the 7.5 wt% Ba/Y_2O_3 was significantly higher than that for the 1 wt% sample. In both catalysts, the oxygen near-edge absorption is greater than that in pure Y_2O_3, which is consistent with the idea that Ba presence causes increased charge deficiency on certain oxygen sites, and this correlates with greater selectivity and activity for C_{2+} production.

CONCLUSIONS

1. There is XANES evidence that Ba loading onto Y_2O_3 effects the step height of the oxygen edge. Increasing Ba loading increases the oxygen near-edge absorption, which is consistent with increased oxygen charge deficiency in the oxygen sublattice.

XANES could therefore be used as a research tool to guide catalyst development by monitoring the catalyst's oxygen charge deficiency.

2. Increasing Ba loading onto Y_2O_3 significantly increases oxidative coupling activity and also increases C_{2+} selectivity. This is consistent with the hypothesis that oxygen charge-deficient sites created by substituting Ba^{2+} into Y^{3+} sites are the active sites for methane C–H bond activation.

3. Formation of $BaCO_3$ by reaction of the Ba/Y_2O_3 with CO_2 in the air inhibits the substitution of Ba into the Y_2O_3 lattice. This was confirmed by XPS and supported by XRD results. Thermally decomposing the $BaCO_3$ will increase the Ba substitution, which is another reason that the catalyst does not become active at lower temperatures.

4. Significant increases in the step height of the oxygen edge are observed when the Ba/Y_2O_3 sample temperature is maintained at 600°C. Higher temperatures facilitate both the increased rate of Ba substitution into the Y_2O_3 lattice and the breakdown of the carbonate phases that hinder this substitution.

ACKNOWLEDGMENTS

We acknowledge M. J. Spangler for the catalyst screening work. We acknowledge the support of the Amoco Corporation and the National Center for Supercomputer Applications for supercomputer time. This work was supported in part by the Department of Energy, Office of Basic Energy Sciences–Materials Sciences Contracts W-31-109-Eng-38 and DE-FG02-85ER4522 and by the Donors of the Petroleum Research Fund, administered by the American Chemical Society.

REFERENCES

1. Driscoll, D. J., and Lunsford, J., *J. Phys. Chem.* **89,** 4415 (1985).
2. Wang, J., and Lunsford,J., *J. Phys. Chem.* **90,** 3890 (1989).
3. Alp, E. E., Campuzano, J. C. Jennings, G., Guo, J., Ellis, D. E., Beaulaigue, L., Mini, S., Zhou, Y., Veal, B. W., and Liu, J. Z., *Phys. Rev. B* **40**(13), 9385 (1989).
4. Johansson, L. I., Allen, J. W., Lindau, I., Hecht, M., and Hagstrum, S. B. M., *Phys. Rev. B* **21,** 1408 (1980).
5. Fano, U., *Phys. Rev.* **124,** 1866 (1961).
6. Vvedensky, D. D., Saldin, D. K., and Pendry, J. B., *Comput. Phys. Commun.* **40,** 421 (1986).
7. Mattheiss, L. F., *Phys. Rev. A* **133,** 1399 (1964).
8. Hermann, F., and Skillman, S., "Atomic Structure Calculations." Prentice–Hall, Englewood Cliffs, NJ, 1963.
9. Pauling, L., "The Nature of the Chemical Bond." Cornell University Press, Ithaca, NY, 1960.
10. Durham, P. J., Pendry, J. B., and Hodges, C. H., *Comput. Phys. Commun.* **25,** 193 (1982).
11. Brydson, R., Sauer, H., Engel, W., Thomas, J. M., Zeitler, E., Kosugi, N., and Kuroda, H., *J. Phys. Condens. Matter* **1,** 797 (1989).
12. Mustre de Leon, J., Rehr, J. J., Zabinsky, S. I., and Albers, R. C., *Phys. Rev. B* **44,** 4146 (1991).
13. Wang, X., and Rez, P., *in* "Proceedings, 4th Annual Meeting of the Electron Microscopy Society of America," p. 128. San Francisco Press, 1987.
14. Thromat, N., Gautier, M., Jollet, F., Duraud, J. P., and LeGressus, C., *Surf. Interface Anal.* **15,** 355 (1990).